Indian Journal of Chemistry
Vol. 62, December 2023, pp. 1239-1246
DOI: 10.56042/ijc.v62i12.2456

Non-linear optical and electronic properties of oxa[n]circulenes: A theoretical insight

Vipin Kumar[a], Raj Kamal[b] & Prabhakar Chetti*[a]

[a] Department of Chemistry, National Institute of Technology (NIT), Kurukshetra 136 119, Haryana, India

[b] Department of Chemistry, Kurukshetra University, Kurukshetra 136 119, Haryana, India

E-mail: chetty_prabhakar@yahoo.com

Received 7 June 2023; accepted (revised) 10 November 2023

In the current work, we have investigated the charge transport and Non-Linear Optical (NLO) characteristics of oxa[n]circulenes. Density functional theory (DFT) and Time dependent density functional theory (TD-DFT) are used to examine optoelectronic and NLO characteristics. TD-DFT calculations are utilized to simulate the absorption energies. Ionization potential (I.P.), electron affinity (E.A.), the frontier molecular orbitals (FMOs) i.e., Highest occupied molecular orbital (HOMO), Lowest unoccupied molecular orbital (LUMO) and HOMO-LUMO gap (E_{ge}) are calculated for the reported molecules. Nuclear independent chemical shift (NICS) values are generated to find aromatic behavior and stability of oxa[n]circulenes. Along with first and second hyperpolarizabilities, optoelectronic properties are also reported for the designed compounds.

Keywords: Oxa[n]circulenes, DFT, TD-DFT, Hyperpolarizabilities, NICS

The circulene family of compounds includes polyaromatic hydrocarbons with fused benzene rings fully saturated on all of the edges and a core ring having fixed number of carbon atoms. The corannulene, a prominent member of this group of compounds, is well recognized for having a form similar to the top piece of C_{60}. Due to its potential to help in the construction of polyhedral molecules like fullerenes, the family has gained the consideration of researchers in the recent years. Additionally, their significant charge delocalization and polarizability imply that they would be intriguing candidates for effective optical and electrical materials.

The planar, aromatic and highly symmetric molecule coronene ([6]circulene) has been carefully synthesized, investigated, and characterized[1,2]. Due of its strong electrical resonance, corannulene possesses intriguing conducting characteristics. Recently developed pleiadannulene ([7]circulene) has a saddle-shaped non-planar structure with blatantly poor symmetry. Numerous theoretical researches have focused on its electrical structure[3]. [8]circulene was successfully synthesized by C. N. Feng[4]. It is a member of the circulene family and is indicated by a center portion of cyclooctatetraene that is completely encircled by phenyl rings. Also, some theoretical investigations[5] have been reported on its structure: to the best of our knowledge, there is no comprehensive analysis. Similarly, Yusuke Matsuo *et al.*[6] reported the syntheses of pentabenzopentaaza[10]circulene. Afshin Dadvand et al. studied heterocirculenes as a new class of organic semiconductor[7] and shown the applications in field effect transistors.

In the present work, we have studied non-linear optical (NLO) and charge transport characteristics of oxa[n]circulenes (n=6-10). NICS calculations are performed to find out the stability of the oxa[n]circulene in terms of aromaticity. 1st and 2nd hyperpolarizability calculations are performed for oxa[n]circulene. All the studied oxa[n]circulenes are given in Scheme 1.

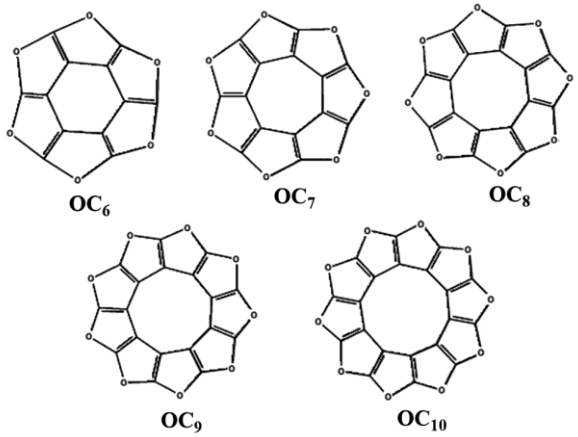

Scheme 1 — All the studied oxa[n]circulenes (n=6-10)

Computational Methodology

All the geometries of oxa[n]circulenes (Scheme 1) are optimized by utilizing Gaussian 16W software[8] with B3LYP/6-311+G (d, p) theoretical level. All the structures are found with no negative frequency on potential energy surface diagram, indicating the stability of the studied oxa[n]circulenes. Using the optimized structures, TD-DFT (TD-B3LYP/6-311+G (d, p))[9,10] investigations was performed on oxa[n]circulenes for absorption properties. Frontier molecular orbital (FMO) analyses were conducted at the same theoretical level. Together with ground state structure, anionic and cationic states were optimized with same theoretical level to facilitate the determination of the charge transport properties.

Further, Ionization potentials (IP) are calculated by using Equations 1, where electron affinities (EA) are calculated by using Equations 2.

$$IP = E^{+}(M_c) - E^{0}(M_0) \quad \ldots (1)$$

$$EA = E^{0}(M_0) - E^{-}(M_-) \quad \ldots (2)$$

here, $E^{0}(M_0)$, $E^{-}(M_-)$ and $E^{+}(M_+)$, denotes the energies of *neutral*, *anionic* and *cationic* form in lowest energy structures, respectively; $E^{+}(M_0)$ / $E^{-}(M_0)$ denotes the energy of the cationic/anionic form with the neutral geometry; $E^{0}(M_-)$ / $E^{0}(M_+)$ denotes energy of neutral molecule with anionic/cationic geometries[10,11].

Results and Discussions

Geometry and stability

The structures of all the studied circulenes are optimized by using Gaussian 16W with B3LYP/6-311+G (d, p) level of theory. Optimized structures of all oxa[n]circulenes with dihedral angles are given in Table 1.

The dihedral angles are –14.3° and –5.2° in oxa[6]-circulene and oxa[10]-circulene, respectively. Table 1 clearly shows that as we are moving from oxa[6]circulene to oxa[10]circulene the geometry is changing from bowl shape to planar. The stability of various molecules is not just dependent on their symmetry; other elements also play a role[12]. One of the elements determining a molecule's stability is its aromatic nature. To know the aromatic nature of the molecule, Nucleus Independent Chemical Shift (NICS) simulations are carried out for the reported circulenes. NICS values aid in figuring out if fused

Table 1 — Optimized structures at B3LYP/6-311+G (d, p) level of theory

Molecules	Optimized Structures
OC_6	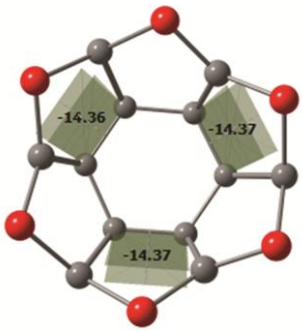
OC_7	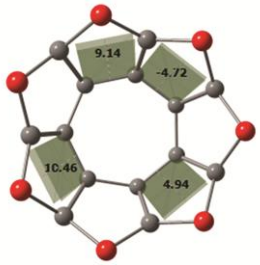
OC_8	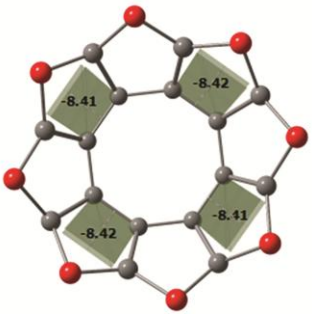
OC_9	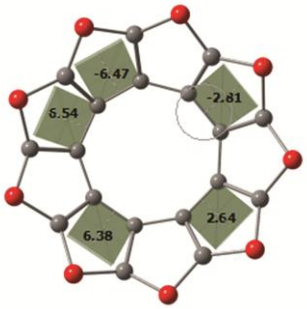
OC_{10}	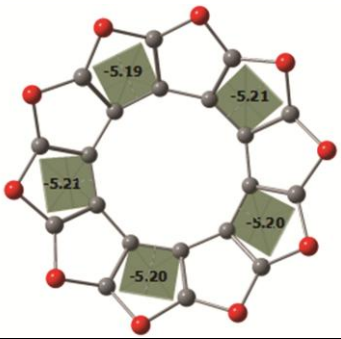

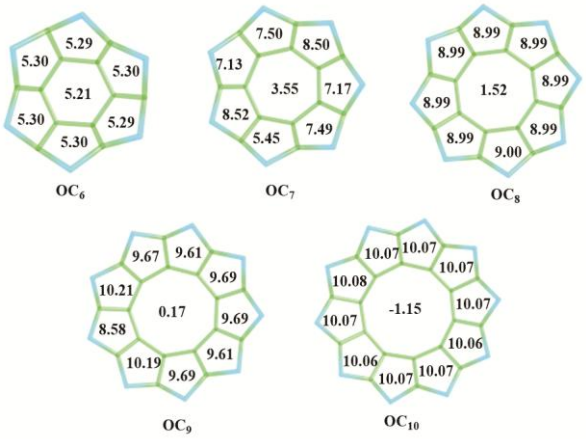

Scheme 2 — Simulated NICS (0) values of circulenes

ring structures are aromatic. Schleyer *et al*. launched NICS in 1996[13]. NICS may be regarded as the negative of magnetic shielding and is a well-known feature of the conjugated electronic system. The NICS (0) values are calculated by entering a dummy atom at the center of the ring. B3LYP/6-311+G (d, p) level is used for NICS calculations and values are analyzed from the obtained output files. Any ring system with a -ve NICS value is aromatic, whereas a +ve NICS value is antiaromatic by nature. Zero NICS values indicates that the ring system is non-aromatic in nature. In our earlier report, we have also described NICS (0) simulations for Benzodithiophene (BDF) isomers and Benzotrithiophene (BTT) oligomers to elucidate stability of the isomers[14,15]. DFT calculated NICS (0) values are shown in Scheme 2. From Scheme 2, it is clearly observed that antiaromatic character of central ring is decreasing with the increase in central ring size from 6-10. From calculated NICS (0) values it is found that Oxa[10]circulene is having aromatic character in central ring. Meanwhile, antiaromatic character of the furan rings is increasing which reflects decrease in delocalization of electrons in the backbone of the molecule.

Absorption Studies

The B3LYP/6-311+G (d, p) optimized structures are used to simulate absorption properties by using TD-B3LYP/6-311+G (d, p) level of theory. Simulated absorption for OC_6 showed a local peak at 427 nm, which is in good agreement with the experimentally measured value of 415 nm[16]. This transition arises from HOMO to LUMO and HOMO-1 to LUMO with low oscillator strength. The theoretical result shows the reliability of method as it is reproducing the same experimental results. However, the absorption maxima are with low intensity in both theoretical and experimental spectra. The calculated absorption energies, Oscillator strength, Major transitions, percentage contribution for oxa[n]circulenes are compiled in Table 2.

The calculated absorption maxima for all the reported molecules ranges from 291 to 594 nm. From Table 2, it is clearly seen that the higher absorption energies are arising mainly due to HOMO to LUMO or HOMO-1 to LUMO molecular transitions with low oscillator strength, suggesting n→л* transition. However, л →л* transitions are arising mainly due to HOMO-1 to LUMO+1, HOMO-2 to LUMO+1, HOMO to LUMO+1 etc. with good oscillator strength. As we move from OC_6 (hexaoxa[6] circulene) to OC_{10} (decaoxa[10]circulene) absorption maxima decreases (Table 2) that suggests decrease in delocalization of electrons in the inside ring of the molecules. The graphical representation of absorption spectra of all the oxa[n]circulene is given in Fig. 1.

Frontier molecular orbitals (FMOs), Electron Affinity (EA) and Ionization Potential (IP)

Frontier molecular orbitals (FMOs) provide details on optical characteristics, electronic transitions, UV-vis absorption, and are crucial in the explanation of a variety of chemical processes in conjugated systems. The HOMO energy of a molecule denotes its capacity to donate electrons (making it a nucleophilic site), and it is closely connected to the IP. The energy of LUMO denotes the inclination to receive electrons (electrophilic site), and its energy is related to the electron affinities. Higher stability, lower reactivity, and lesser polarizability are often characteristics of higher E_{ge}. Graphical representation of FMOs with E_{ge} is shown in Fig. 2. FMOs of all the oxa[n]circulenes are tabulated in Table S1.

The calculated HOMO and LUMO values are ranges from –6.60 eV to –6.86 eV and –2.22 eV to –3.97 eV, respectively. The E_{ge} is in-between 2.89 eV to 4.38 eV. Table 3 lists all of the HOMO, LUMO, and E_{ge} energies. From Table 3, it is clearly seen that as we move from OC_6 to OC_{10}, the E_{ge} is increasing considerably, suggesting a decrease in the delocalization of electrons from one ring to another.

For each molecule, the capacity to inject holes and electrons is mostly determined by the molecular EA and IP. IP and EA can forecast how well organic

Table 2 — Absorption (λ_{max}), Oscillator strength (f), Major Transitions (M.T.), % Contribution at TD-B3LYP/6-311+G (d, p) level of theory

Molecule	States	λ_{max} (nm)	f	M.T.	%Ci
OC_6	S1	594	0.0024	H → L	100
	S2	593	0.0024	H-1 → L	100
	S5	427	0.0168	H-2 → L+2	20
				H-1 → L+1	39
				H → L+2	39
	S6	427	0.0168	H-2 → L+2	18
				H-1 → L+1	18
				H-1 → L+2	21
				H → L+1	21
				H → L+2	18
	S7	395	0.0031	H-1 → L+2	49
				H → L+1	49
	S8	335	0.1632	H-2 → L+1	72
				H-1 → L+2	10
				H → L+1	10
	S9	335	0.1631	H-2 → L+2	72
				H-1 → L+1	10
				H → L+2	10
	S10	292	0.0238	H-4 → L	86
OC_7	S2	507	0.0007	H-1 → L	100
	S3	490	0.0004	H-2 → L	99
	S4	432	0.0034	H-3 → L	94
	S5	389	0.0041	H-1 → L+2	26
				H → L+1	74
	S6	382	0.0415	H-2 → L+1	53
				H → L+2	29
	S7	378	0.0001	H-2 → L+1	40
				H-1 → L+1	16
				H → L+2	43
	S8	370	0.0004	H-2 → L+2	41
				H-1 → L+2	40
				H → L+1	14
	S9	366	0.0645	H-2 → L+2	55
				H-1 → L+2	25
	S10	344	0.0012	H-3 → L+2	29
				H-1 → L+1	43
				H → L+2	24
OC_8	S1	427	0.0011	H → L	98
	S2	427	0.0011	H-1 → L	98
	S8	346	0.0001	H-1 → L+1	31
				H-1 → L+2	19
				H → L+1	17
				H → L+2	33
	S9	334	0.0322	H-2 → L+1	23
				H-2 → L+2	12
				H → L+3	59
	S10	334	0.0322	H-2 → L+1	12
				H-2 → L+2	23
				H-1 → L+3	59

(contd.)

Table 2 — Absorption (λ_{max}), Oscillator strength (f), Major Transitions (M.T.), % Contribution at TD-B3LYP/6-311+G (d, p) level of theory (*contd.*)

Molecule	States	λ_{max} (nm)	f	M.T.	%Ci
	S2	384	0.0019	H-1 → L	98
	S4	358	0.003	H-3 → L	93
	S5	343	0.0081	H-3 → L+1	30
				H → L+2	49
	S6	337	0.0146	H → L+1	83
	S7	332	0.0011	H-2 → L+1	10
				H-1 → L+1	47
				H → L+2	38
	S8	332	0.0127	H-1 → L+2	82
	S9	318	0.0053	H-2 → L+1	77
				H-1 → L+1	19
	S10	315	0.0103	H-3 → L+1	57
				H → L+3	34
OC_{10}	S1	330	0.0014	H → L	94
	S2	330	0.0013	H-1 → L	94
	S6	307	0.0009	H-4 → L	73
				H-1 → L+1	11
				H → L+2	11
	S9	291	0.0466	H-3 → L+1	11
				H-3 → L+2	27
				H-2 → L+1	28
				H-2 → L+2	11
	S10	291	0.0471	H-3 → L+1	28
				H-2 → L+1	11
				H-2 → L+2	27

* Transitions with zero oscillator strengths are omitted.

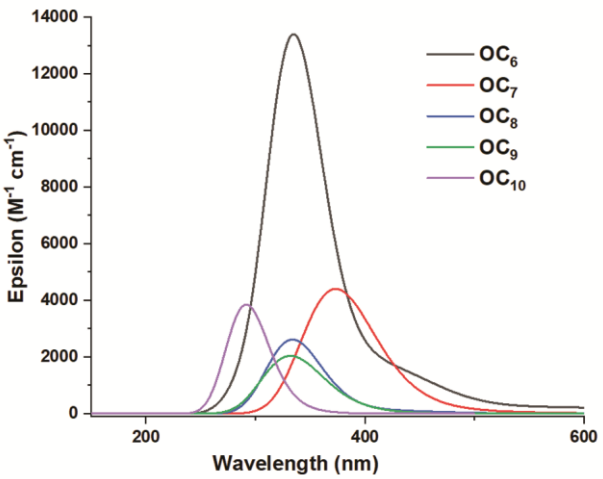

Fig. 1 — Absorption spectra of studies oxa[n]circulene

electronic materials would transport electrons and holes. IP, which is the energy needed to effectively inject a hole into a molecule's HOMO when an electron is withdrawn, should be as low as possible. The amount of energy needed by a molecule to get electrons is measured by its electron affinity (EA), and a molecule may more easily obtain electrons if its EA value is larger. The calculated IP ranges 7.81 to 8.16 eV. While, the calculated EA ranges 1.05 to 2.58 eV.

Molecular Electrostatic Potential (MEPs)

The MEP is very helpful for visualizing the distribution pattern of electron clouds, relative polarity (dipole moment), interactions between H-bonds[17], and possible electrophilic-nucleophilic sites[18,19]. Darkest blue > cyan > green > yellow > orange > darkest red are the sequence in which the electrostatic potential decreases[20]. In MEP, the colors reddish-orange, blue, and green are used to represent the regions of neutral electrostatic potential and the precincts of maximum negative electrostatic potential and maximum positive electrostatic potential, respectively, where electrophilic reactions would occur preferentially and nucleophilic reactions would preferentially occur. As we move from OC_6 to OC_{10} red color on central ring gets fade which indicates the nucleophilic character decreases with increase in central ring size. The molecular electrostatic potential (MEPs) maps for all the studied molecules are given in Table 4.

Table 3 — Calculated Ionization potential, Electron affinities, HOMO, LUMO and E_{ge}

Molecules	IP (eV)	EA (eV)	HOMO (eV)	LUMO (eV)	E_{ge} (eV)
OC_6	8.16	2.58	–6.86	–3.97	2.89
OC_7	8.05	2.29	–6.67	–3.61	3.06
OC_8	7.90	1.75	–6.60	–3.03	3.57
OC_9	7.85	1.63	–6.52	–2.69	3.83
OC_{10}	7.81	1.05	–6.60	–2.22	4.38

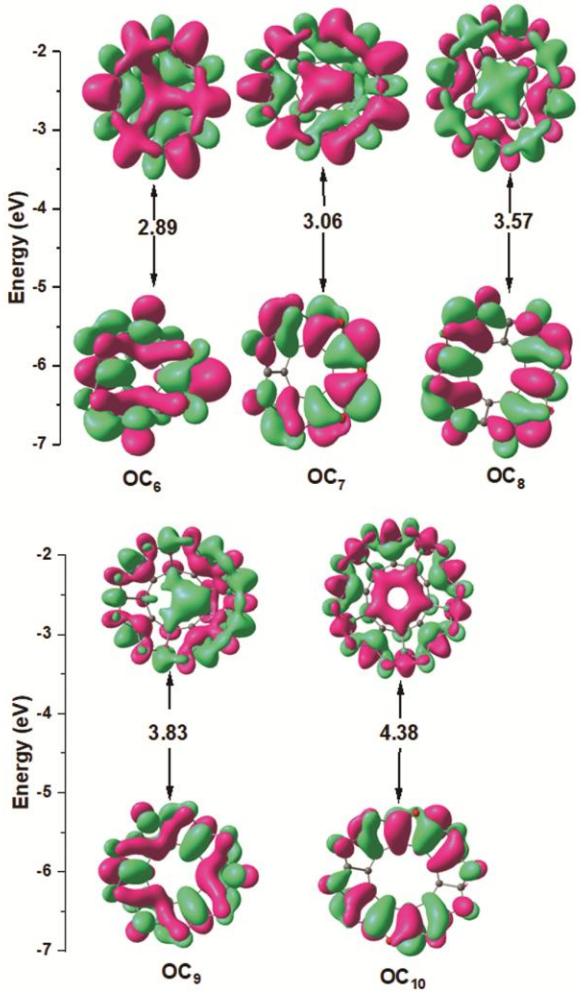

Fig. 2 — FMOs with HOMO-LUMO gap for oxa[n]circulene (isosurface value = 0.02)

Dipole moment and Non-linear optical properties

The separation of two opposing electrical charges is measured by a dipole moment. The dipole moment of a molecule has significant contributions to the understanding of complex molecule structure, particularly in the organic realm. The dipole moment's magnitude is proportional to the charge times the separation distance between the charges, and it is directed from negative charge to positive charge:

Table 4 — Molecular electrostatic potential (MEP)at B3LYP/6-311+G (d, p) level of theory

Molecules	MEP Spheres
OC_6	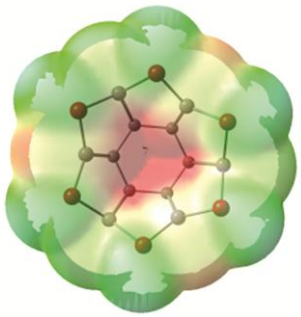
OC_7	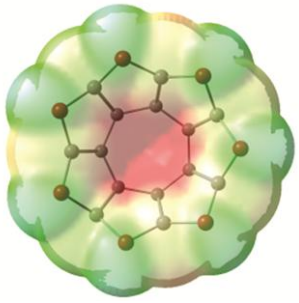
OC_8	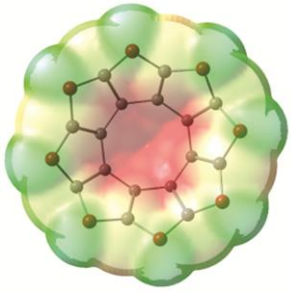
OC_9	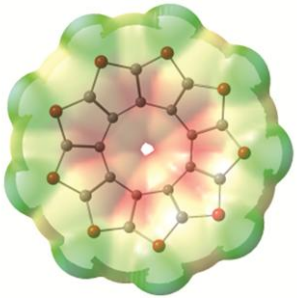
OC_{10}	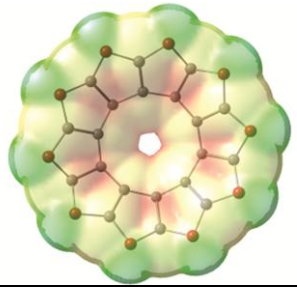

Table 5 — DFT calculated 1st hyperpolarizabilities, 2nd hyperpolarizabilities and Dipole moment (μ)

Molecules	First hyperpolarizability (β) 10^{-26}	Second hyperpolarizability (γ) 10^{-35}	Dipole moment (μ) (in Debye)
OC_6	1.56	3.11	1.54
OC_7	0.37	0.74	1.36
OC_8	0.06	0.11	1.18
OC_9	0.12	0.02	1.03
OC_{10}	0.06	0.12	0.78

μ = q * r. The calculated dipole moment for oxa[n]circulenes are given in Table 5. From Table 5, with the increase in the size of central ring the dipole moment decreases and E_{qe} increases, suggesting less delocalization of electrons in backbone of molecules.

In signal processing, communication technologies, optical switches, and optical memory systems, NLO compounds are often utilized. The multidirectional charge transfer that occurs in the various pieces of the molecule determines the optical nonlinearities in molecules. A molecule must transfer charges in the excited state in order for it to be optically non-linear, according to the generalized Mulliken-Hush analysis. For enriching hyperpolarizability, it is known that in addition to boosting donor or acceptor strength, as per two state model, one need also keeps an eye on the delocalization or localization of the electrons in two states[21, 22]. At a suitable location where the wave functions defining two states appreciably overlap, the optimal hyperpolarizability can be attained[23]. It has been noted that in an organic push-pull system, HOMO and LUMO levels must overlap across the conjugated bridge in order to attain strong hyperpolarizability[24,25].

First hyperpolarizability (β) depends on the charge transfer dipole moment ($\Delta\mu_{ge}$), square of the transition dipole moment (μ_{ge}), and HOMO-LUMO gap (E_{ge})[26] as in equation (3)[27], Oudar's[28,29] two-state model explains the non-linear behavior of organic molecules with enhanced hyperpolarizabilities.

$$\beta \propto (\mu_{ge})^2 \Delta\mu_{ge}/(E_{ge})^2 \quad \text{... (3)}$$

The calculated value of first hyperpolarizabilities of the investigated oxa[n]circulenes are considerably greater than that of p-nitroaniline[27].

Further, to apprehend the third-order NLO efficiency of designed molecules second hyperpolarizability (γ) can be calculated by using eq. (4)[30]:

$$\langle\gamma\rangle=(1/5)[\gamma xxxx+\gamma yyyy+\gamma zzzz+2(\gamma xxyy+\gamma xxzz+\gamma yyzz)] \quad \text{... (4)}$$

The calculated 1st and 2nd Hyperpolarizabilities for studied oxa[n]circulene is of order 10^{-26} and 10^{-35} esu, respectively and presented in Table 5. From Table 5, it is observed that the hyperpolarizability values increases with the decrease in E_{qe}.

According to the most recent research, our designed molecules have the ability to respond to NLOs and can be utilized to create intelligent non-linear optical materials.

Conclusions

In conclusion, in the present work we have studied theoretically oxa[n]circulenes for possible linear and non-linear optical properties. NICS calculations showed that the aromatic character of central ring of the circulene is increasing with the increase in the size of the central ring. Absorption properties are showing two types of transitions, i.e.: л →л* and n →л* transitions. FMO analysis shows HOMO-LUMO gap is in-between 2.89 to 4.38 eV. HLG increases with increasing ring size, which suggests there is lesser delocalization of electrons in oxa[n]circulenes. Calculated dipole moment ranges from 0.78 to 1.54 Debye. Further, 1st and 2nd Hyperpolarizabilities for studied oxa[n]circulene is of order 10^{-26} and 10^{-35} esu.

Hence, these studied oxa[n]circulenes are suitable candidate for NLO properties and can be possibly used in NLO device fabrications.

Supplementary Information

Supplementary information is available in the website http://nopr.niscpr.res.in/handle/123456789/58776.

Conflict of interest

No potential conflict of interest was reported by the author(s).

References

1 Newman M S, *J Am Chem Soc*, 62 (1940) 1683.
2 Yamamoto K, Harada T, Nakazaki M, Nakao T, Kay Y, Harada S & Kasai N, *J Am Chem Soc*, 110 (1988) 3578.
3 Shen M, Ignatyev I S, Xie Y & Schaefer H F, *J Phys Chem*, 97 (1993) 3212.
4 Feng C N, Kuo M Y & Wu Y T, *Angew Chem Int Ed*, 52 (2013) 7791.

5 Liljefors T & Wennerstrom O, *Tetrahedron*, 33 (1977) 2999.
6 Matsuo Y, Kise K, Morimoto Y, Osuka A & Tanaka T, *Angew Chem Int Ed*, 134 (2022) e202116789.
7 Dadvand A, Cicoira F, Chernichenko K Y, Balenkova E S, Osuna R M, Rosei F, Nenajdenkoc V G & Perepichka D F, *Chem Commun*, 42 (2008) 5354.
8 M. J. Frisch, G. W. Trucks, H. B. Schlegel, G. E. Scuseria, M. A. Robb, J. R. Cheeseman, G. Scalmani, V. Barone, G. A. Petersson, H. Nakatsuji, X. Li, M. Caricato, A. V. Marenich, J. Bloino, B. G. Janesko, R. Gomperts, B. Mennucci, H. P. Hratchian, J. V. Ortiz, A. F. Izmaylov, J. L. Sonnenberg, D. Williams-Young, F. Ding, F. Lipparini, F. Egidi, J. Goings, B. Peng, A. Petrone, T. Henderson, D. Ranasinghe, V. G. Zakrzewski, J. Gao, N. Rega, G. Zheng, W. Liang, M. Hada, M. Ehara, K. Toyota, R. Fukuda, J. Hasegawa, M. Ishida, T. Nakajima, Y. Honda, O. Kitao, H. Nakai, T. Vreven, K. Throssell, J. A. Montgomery Jr., J. E. Peralta, F. Ogliaro, M. J. Bearpark, J. J. Heyd, E. N. Brothers, K. N. Kudin, V. N. Staroverov, T. A. Keith, R. Kobayashi, J. Normand, K. Raghavachari, A. P. Rendell, J. C. Burant, S. S. Iyengar, J. Tomasi, M. Cossi, J. M. Millam, M. Klene, C. Adamo, R. Cammi, J. W. Ochterski, R. L. Martin, K. Morokuma, O. Farkas, J. B. Foresman, D. J. Fox, Gaussian 16, Revision B.01, Gaussian, Inc., Wallingford CT, 2016.
9 Becke A D, *J Chem Phys* 98 (1993) 5648.
10 Lee C, Yang W & Parr R G, *Phys Rev B*, 37 (1988) 785.
11 Tripathi A, Kumar V & Chetti P, *J Photochem Photobiol A: Chemistry*, 426 (2022) 113738.
12 Tripathi A & Chetti P, *J Chin Chem Soc*, 66 (2019) 891.
13 Schleyer P V R, Maerker C, Dransfeld A, Jiao H & Hommes N J R van E, *J Am Chem Soc*, 118 (1996) 6317.
14 Kumar V, Koudjina S, Verma P & Chetti P, *Spectroch Acta Part A: Mol and Biomol Spectro*, 290 (2023) 122266.
15 Tripathi A & Chetti P, *J Mol Sim*, 46 (2020) 548.
16 Demircioğlua Z, Kaştaş G, Kaştaş Ç A & Frank R, *J Mol Str*, 1191 (2019) 129.
17 Murray J S & Politzer P, *Wiley Interdisci Reviews: Comp Mol Sci*, 1 (2011) 153.
18 Nielsen C B, Brock-Nannestad T, Reenberg T K, Hammershøj P, Christensen J B, Stouwdam J W & Pittelkow M, *Chem Eur J*, 16 (2010) 13030.
19 Tripathi A, Ganjoo A & Chetti P, *Solar Energy*, 209 (2020) 194.
20 Marder S R, Kippelen B, Jen A K Y & Peyghambarian N, *Nature*, 388 (1997) 845.
21 Zerner M C, Fabian W M FDworczak, R, Kieslinger D W, Kroner G, Junek H & Lippitsch M E, *Int J Quantum Chem*, 79 (2000) 253.
22 Kanis D R, Ratner M A & Marks T J, *Quantum chemical aspects Chem Rev*, 94 (1994) 195.
23 Yoshimura T, *Phys Rev B*, 44 (1991) 13175.
24 Yoshimura T, *Appl Phys Lett*, 55 (1989) 534.
25 Ward J F, *Rev Mod Phys*, 37 (1965) 1.
26 Oudar J L, *J Chem Phys*, 67 (1977) 446.
27 Oudar J L & Person H L, *Opt Commun*, 15 (1975) 258.
28 LeCours S M, Guan H W, DiMagno S G, Wang C H & Therien M J, *J Am Chem Soc*, 118 (1996) 1497.
29 Oudar J L & Chemla D S, *J Chem Phys*, 66 (1977) 2664.
30 Karakas A, Ceylan Y, Karakaya M, Taser M, Terlemez B B, Eren N, El Kouari Y, Lougdali M, Arof A K & B. Sahraoui, *Open Chem*, 17 (2019) 151.